Name of Journal: *MedMat*

Manuscript Type: Original Article

TiB particle-stimulated nucleation of recrystallization behavior in a novel Ti-Mo-Fe biomedical titanium alloy

Short title: Recrystallization in a novel Ti-Mo-Fe biomedical alloy

Hanzhao Qin, Li Ma, Chenglin Li*

School of Power and Mechanical Engineering, Wuhan University, Wuhan 430072, Hubei Province, China

*Corresponding author: School of Power and Mechanical Engineering, Wuhan University, No. 8, South Donghu Road, Wuchang District, Wuhan 430072, Hubei Province, China
Email: lichenglin211@whu.edu.cn

ABSTRACT

Background: Beta titanium alloys are widely used in biomedical implants because of their high strength and low modulus, for example, Ti-Mo-Fe based alloys exhibit superior mechanical properties and are good condidates for bone implants. A novel biomedical Ti-9.2Mo-2Fe-0.1B (wt.%) beta titanium alloy was developed for biomedical purpose. Therefore, in this study, we investigated the microstrucural evolution of the novel alloy in the early stage of annealing to understand its static recrystallization behavior.

Methods: The alloy samples were cold compressed and then subjected to a beta solution treatment for a short time. The microstructural and textural evolution at the early-stage of static recrystallization were investigated by using electron backscatter diffraction (EBSD) technique.

Results: EBSD observations reveal that new grains/subgrians are nucleated in particles deformation zones that were the beta matrix and twins surrounded with TiB particles.

High angle grain boundaries were formed between the recystallized grains and subgrains via various lattice rotation. The recrystallized microstructures exhibited weakened textures in the beta solution-treated Ti-9.2Mo-2Fe-0.1B alloy.

Conclusions: The PSN mechanism is the main recrystallization mechanism in the early stage of static recrystallization. Multiple grains/subgrains are nucleated in the matrix and twins in the vicinty of TiB particles by the lattice rotation. The random rotation leads to formation of large angle grain boundaries and weaken recystallization textures.

Keywords: Biomedical titanium; Grain refinement; Particle-stimulated nucleation; Recrystallization

INTRODUCTION

Titanium and its alloys have been increasingly used for the fabrication of orthopedic implants because of their good fatigue resistance, excellent *in vivo* corrosion resistance, and low elastic modulus.[1,2] The low modulus is believed to reduce the effect of stress-shielding on the bone as well as exhibit an increased fracture toughness as compared to an alpha-beta alloy of equivalent aging.[3,4]

Ti-9.2Mo-2Fe alloy is a novel low-cost metastable beta titanium alloy that was designed based on the Bo-Md method.[5,6] The alloy in a solution treated state exhibits an ultimate tensile strength of 900 MPa, an elastic modulus of 80 GPa, and a ductility of 30%−40%, because of the coexistence of multiple deformation mechanisms, i.e., dislocation slip, twinning and stress-induced martensite transformation.[7,8] The high ductility at room temperature enables to manufacture of products in the form of sheets or pipes through cold deformation such as rolling, drawing. Subsequent annealing or solution treatment then can generate refined grain sizes to obtain superior mechanical properties.[9–11] For example, Cai *et al.*[12] reported that the β grain size of Ti-16V-3.5Al-3Sn alloy after cold rolling plus beta solution treatment can be refined to 1.3–30 μm. The grain refinement of β phase also improved the plasticity of the titanium alloy after aging.

However, beta-titanium alloys after cold rolling generally exhibit a strong texture that is inherited from their recrystallization textures of beta grains, which are determined by grain boundary bulging or grain subdivision mechanisms. This inherited texture typically causes anisotropic properties. Zhang *et al.*[13] reported that the TiCx particles can promote the beta grain recrystallization during hot deformation in a Ti–35V–15Cr–

0.3Si–0.1C beta titanium alloy through the particle stimulated nucleation (PSN). PSN mechanism is an effective nucleation behavior which promotes the recrystallization and weaken the texture of recrystallized microstructure in steel, Al alloys, and Mg alloys.[14] Previous studies reported that TiB particles can produce the PSN behavior in Ti-2Al-9.2Mo-2Fe-0.1B alloy in terms of dynamic recrystallization during hot deformation.[15,16] However, the PSN behavior of TiB particles in this newly-developed biomedical titanium alloy during static recrystallization has not been investigated yet.

In this work, Ti-9.2Mo-2Fe alloy modified with 0.1wt.% boron was used. The samples were cold compressed and then subjected to solution treatment at 850 for a short time to investigate the early stage of recryllization. PSN behavior of TiB particles, static recrystallization behavior and texture evolution during beta solution treatment were investigated.

MATERIALS AND EXPRIMENTAL

An ingot with a dimension of 110 mm in diameter and 500 mm in length was prepared using double vacuum arc remelting. Ti-32Mo, MoFe, and FeB20 master alloys were used as alloying additives to reduce the alloying cost and, to obtain a homogenous composition. The beta transus temperature of this alloy was 790 ± 5 ℃. The ingot was solution treated at 850 ℃ for 1 h, followed by water quenching (WQ), to obtain a single β-phase microstructure of fully beta grains.

Cylindrical samples of Φ5 mm × 5 mm were machined from the solution treated ingot for room-temperature compression tests. The cylindrical axes of the samples parallelled to the longitudinal direction of the ingot. Compression tests were conducted at room temperature using a SANS universal testing machine under a load speed of 0.2 mm/min, corresponding to a strain rate of 6×10^{-4} /s. The samples were compressed with reduction in heights of 30% and 50%. The deformed samples were then solution treated at 850 ℃ for 2 min under an argon atmosphere, using a rapid thermal processing furnace with a heating rate of about 200 ℃/s and a cooling rate of about 100 ℃/s.

The samples for microstructural observations were mechanically ground and polished. The finished samples were etched in a Kroll etchant for optical microscope (OM) observation using an OLYMPUS BX51. Electron backscattering diffraction (EBSD) and electron channeling contrast imaging (ECCI) were used to characterize grain structures and deformed structures, respectively. EBSD observations were carried out

by using a field-emission scanning electron microscope (FE-SEM, JEOL 7001F, 20 kV) and an Aztec EBSD system. A working distance of 15 mm was used. A step size of 0.3 μm was used for the EBSD mappings.

RESULTS AND DISCUSION

As-deformed structure

Figure 1 shows the deformed microstructures of the samples after compression with two reductions of 30% and 50%. It is observed that TiB particles are mainly located at the β grain boundaryies, as indicatd by the arrows in Figure 1a and b. After deformtion, the TiB particles are broken and exhibit a cluster morphology, as shown in Figure 1a and 1b. Meanwhile, some white zones are surrounded by TiB particles, which indicates that distortion enery was stored around the TiB particles after deformation. A plenty of bands are observed in the sample deformed with 30% reduction, as shown in Figure 1a. These bands exhibite the same direction in most of the beta grains, indicating of single slip or twinning. With increasing reduction to 50%, intersection of bands occurrs in the beta grains in the compressed sample, as shown in Figure 1b, indicating of activations of multiple slips or twinnning.

EBSD kernel average misorientation and image quality map in Figure 1c reveals the microstructural details of a sginle β grain in the 30% deformed sample. As shown in Figure 1c, higher misorientations are observed in the vicinity of the twin boundaries, as well as the regions near TiB particles. Particles deformation zones (PDZ) are formed in the vicinity of the TiB particles. Line scans of misorientation in the regions near the TiB particles are shown in Figure 1f. It is observed that the regions close to the particles exhibit higher misorentations, which reach values of 5−9°. This indicates that high density of dislocations are progressively acumulated around the TiB particles during deformation. The corresponding pole figures of one band and neighbor matrix on the lower right is shown in Figure 1d. It is obvious that the they correpond to {332}<113> twinning, the misorentation between the band and matrix (from A to B in Figure 1c) is approximately 50°, as shown in Figure 1e. $\{332\}_{\beta}<113>_{\beta}$ is a typical twinning in beta titanium alloy[8,17] because of the low stability of beta phase.[5] As a result, in addition to dislocation slip, twinnning is the dominant deformation mechansim in the alloy deformed at room temperature.

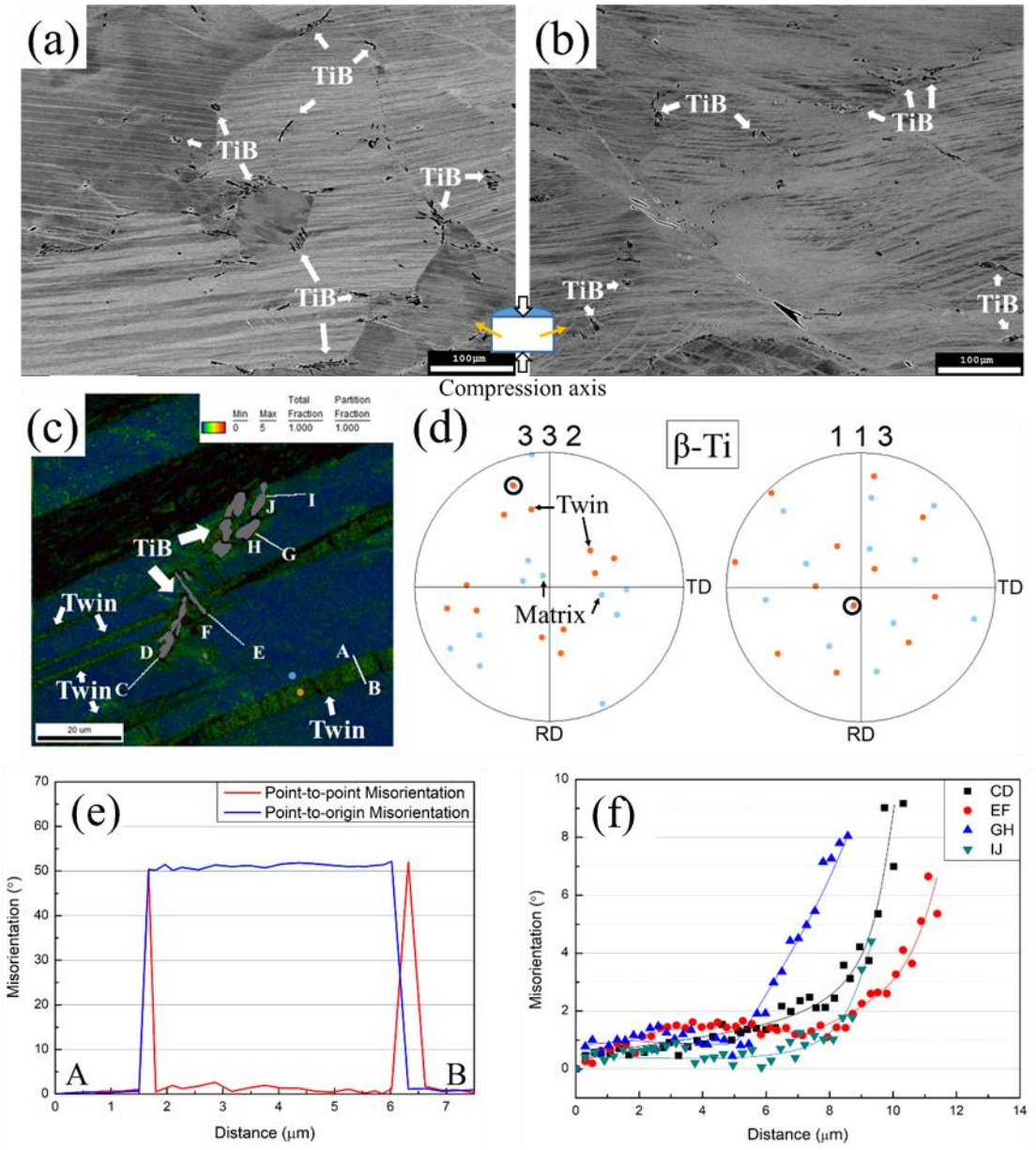

Figure 1. Electron channeling contrast (ECC) images of the compressed samples with reductions of (a) 30% and (b) 50%. (c) Kernel Average Misorientation and image quality map of a deformed grain zone with TiB particles in the 30% deformed sample. (d) $\{332\}_{\beta}$ and $<113>_{\beta}$ pole figures of the twinined zone and matrix in (c). (e) Misorientation profiles from point A to B between twin and matrix in (c). (f) Misorientation profiles along the indicated directions in the deformation zone surrounding the TiB particels in (c).

Recrystallization during following solution treatment

Figure 2 shows the microstructures of the 30% deformed sample after solution treatment for a short time of 2 min. The sample exhibits a typical partially recrystallized

structure, where large original grains (grayscale) and some recrystallized grains (whitescale) coexist, as shown in Figure 2a. Most of the recrystallized grains are originated within initial beta grains, appearing to be associated with the TiB particles. It indicates that the regions surrounding with TiB particles can provide more nucleation sites and higher driving force for recrystallization at the initial stage of solution treatment. The PSN mechanism dominates the nucleation at the early stage of recrystallization in the alloy.

EBSD map in Figure 2b shows the microstrutural details of a region having TiB particles. It is clearly observed that the recrystallized grains are nucleated and grow surrounding TiB particles. The TiB particle sizes are appriximately 1–2 μm. A few new grain are nucleated around TiB particles, i.e., Grain 1–4 formed from the same TiB particle, indicating that some subgrains with various orientations are generated in such one PDZ. Therefore, the PSN mechanism is an efficient nucleation way of recrystallization in titanium alloys. The boundary misorientation angles of the new grains are shown in Figure 2c. Grains 6 and 9 are surrounded by various boundaries of different misorientation angles with matrix. During the beta solution treatment, some subgrains are formed in the PDZ of TiB particles by the lattice rotation with different orientations, e.g. grain 9 and subgrain 10 in Figure 2d. Then, these subgrains are grown up by the boundary migrations drived by the dislocation annihilation in the PDZ. When the different subgrains swallow the matrix between each other, a high angle grain boundary is formed between these subgrains, i.e., the boundary E (about17° of the misorientation angle) in Figure 2d. Although the misorientation of boundaries between the subgrain and matrix is only less than 15°, for example, the boundary D of the subgrain 9 and the boundary F of subgrain 10 are 12° and 8°, respectively. As such, the misorientations between the recrystallized grains are higher than that of recrystallized grain and matrix, likewise grain 1–6 in Figure 2c.

Some recrystallization grains (Grain 3 and 7) are surround by the boundaries near 60° of misorientation angle with the initial beta grain matrix, as shown in Figure 2c. Meanwhile, the misorientation between grain 7 and the T2 twin is 28.5°, and misorientation between grain 3 and the T1 twin is about 25.7°. It means these grains might be formed in the twins beside TiB particles, causing the large misorientation between recrystallized grains with matrix.

The pole figures of PSN grains and original beta grains are shown in Figure 2f. All the

PSN grains have the same crystal plane with the original beta grains, which also indicates the PSN grains are nucleated through the lattice rotation of original grains in the PDZ. The crystal planes of each PSN grains are also randomly distributed, indicating random orientaions of the PSN grains.

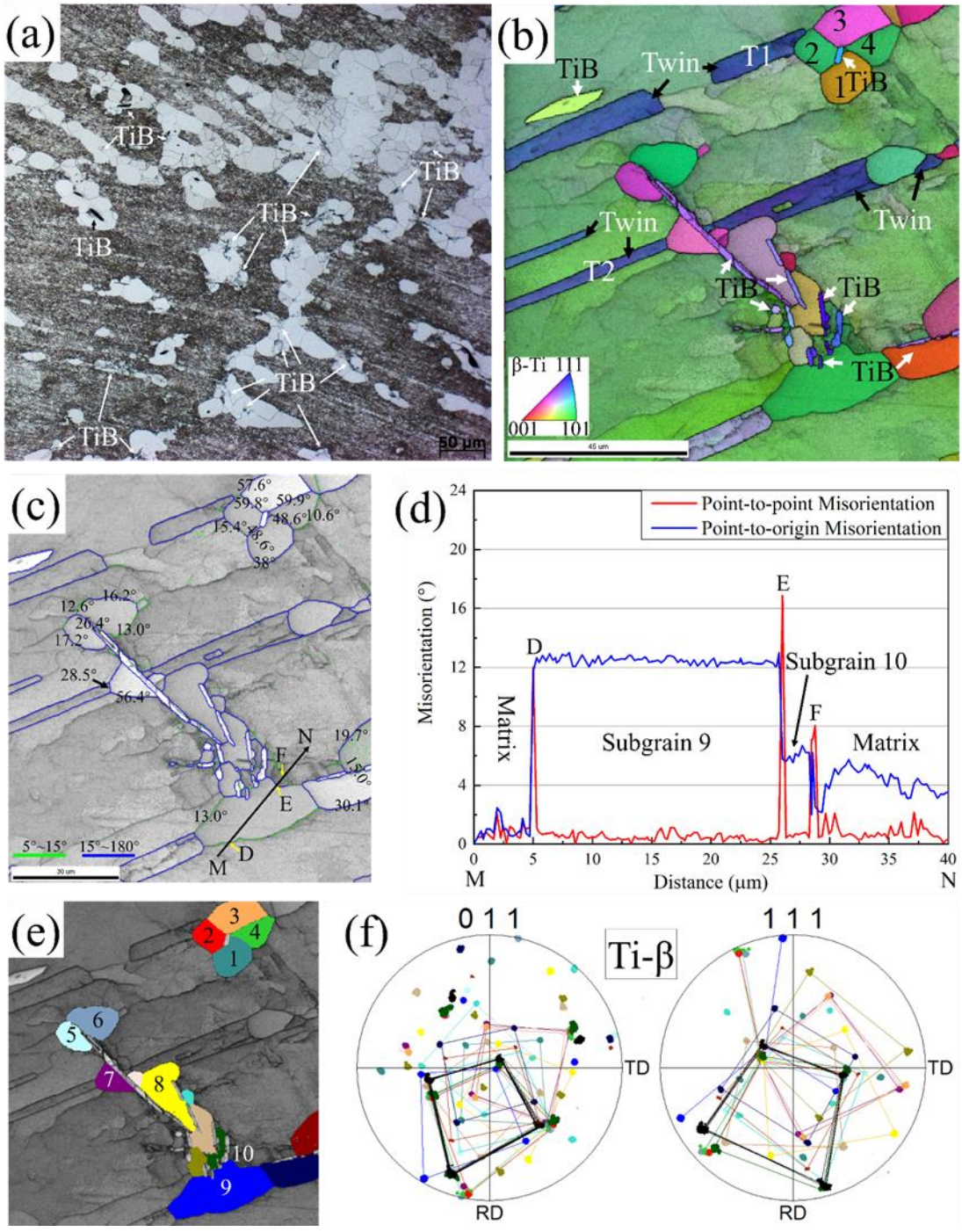

Figure 2. (a) Optical microscope (OM) images showing the 30% deformed sample followed by a solution treatment at 850℃ for 2 min. (b) Inverse pole figure (IPF) map of the TiB particles with recrystallized grains. (c) boundaries misorientation angles of

recystallized grains surrounding TiB particles in (b). (d) misorientation profile along the line marked ‘MN’ line in (c). (e) Image quality map and colored grains of an area of interest in (c). (f) (011) and (111) Pole Figure (PF) maps of recystallized grains (same color in (e)) and the original beta grains (black points) .

Figure 3 shows the microstuctures of the 50% deformed alloy followed by solution treatment for 2 min. Most of the initial beta grains are recrystalled, only a few areas are unrecrystallized, as indicated by the circles in Figure 3a. The recrystallized strucrture showed an equiaxed morphology and a refined grain size of approximately 23 ± 8 μm. In addition, TiB particles are mainly observed at the newly-developed grain boundaries, as indicated by the arrows in Figure 3a and 3b. These areas also exhibited finer size of grains than other areas, which indicates that the PSN behavior by TiB particles is a very effective mechanism during the static recrystallization in beta titanium alloys, as shown in Figure 3a and 3b. On the other hand, the pinning effect of TiB particles may also have an influence on the grain growth.[18] The (001) and (011) pole figures of the recrystallized grains in Figure 3b are shown in Figure 3c. All the crystal planes in each recrystallized grain are randomly distributed in the pole figure, and there are no preferred crystallographic orientation in the recrystallization grains. It indicates that the PSN mechanism can also weaken the texture of static recystallization microstructure in the alloy, as shown in Figure 3d.

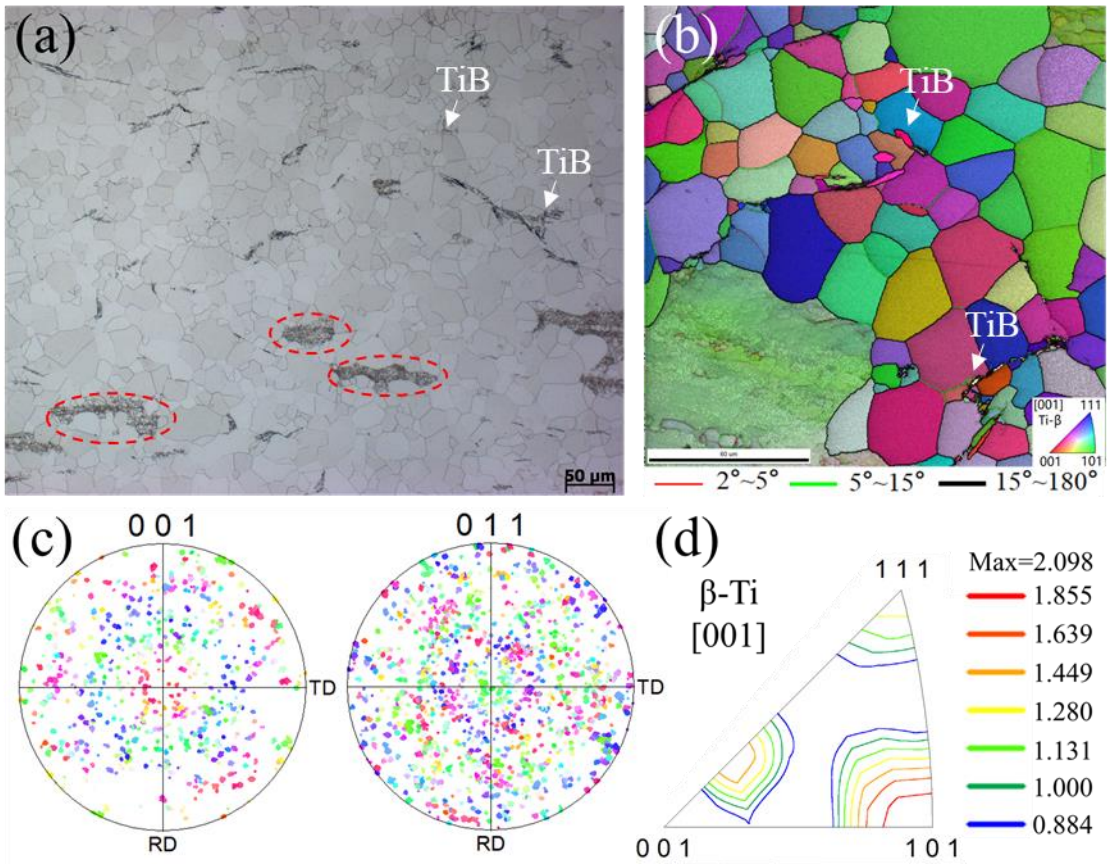

Figure 3. (a) Optical microscope (OM) and (b) Inverse pole figure (IPF) of the 50% deformed sample followed by a beta solution treatment at 850℃ for 2 min. (c) pole figures and (d) inverse pole figure of the recrystallized grains in (b).

CONCLUSIONS

In this work, we investigated the static recrystallization behavior of the cold compressed novel metastable beta Ti-9.2Mo-2Fe-0.1B biomedical titanium alloy at the early stage of beta solution treatment. The PSN mechanism is the main recrystallization mechanism in the early stage of static recrystallization. Multiple grains/subgrains are nucleated in the matrix and twins in the vicinty of TiB particles by the lattice rotation. The rotation is random and leads to large angle grain boundary formation between different recrystallized grains. Moreover, the texture of recystallized grains is weaken due to random lattice rotation.

Source of Funding

None.

Conflict of Intrests

None.

REFERENCES

1. Fan D, Yi Z, Feng X, Tian W, Xu D, Cristino Valentino AM, *et al.* Antibacterial property of a gradient Cu-bearing titanium alloy by laser additive manufacturing. Rare Met 2022;41:580–593.

2. Yang H, Zhu M, Wang J, Ma C, Zhou X, Xing H, *et al.* Optimization of mechanical and antibacterial properties of Ti-3wt%Cu alloy through cold rolling and annealing. Rare Met 2022;41:610–620.

3. Meng Q, Xu J, Li H, Zhao C, Qi J, Wei F, *et al.* Phase transformations and mechanical properties of a Ti36Nb5Zr alloy subjected to thermomechanical treatments. Rare Met 2022;41:209–217.

4. Meng Q, Li H, Zhao C, Ma W, Wei F, Sui Y, *et al.* Synchrotron X-ray diffraction characterization of phase transformations during thermomechanical processing of a Ti38Nb alloy. Rare Met 2021;40:3269–3278.

5. Li C, Lee D, Mi X, Ye W, Hui S, Lee Y. Phase transformation and age hardening behavior of new Ti-9.2Mo-2Fe alloy. J Alloys Compd 2013;549:152–157.

6. Li C, Lee D, Mi X, Ye W, Hui S, Lee Y. Effect of Al Addition on ω Precipitation and Age Hardening of Ti-Al-Mo-Fe Alloys. Metall Mater Trans A 2016;47:2454–2461.

7. Li C, Mi X, Ye W, Hui S, Lee D, Lee Y. Influence of heat treatment on microstructure and tensile property of a new high strength beta alloy Ti-2Al-9.2Mo-2Fe. Mater Sci Eng A 2013;580:250–256.

8. Gutierrez-Urrutia I, Li C, Emura S, Min X, Tsuchiya K. Study of {332}<113> twinning in a multilayered Ti-10Mo-xFe (x = 1–3) alloy by ECCI and EBSD. Sci Technol Adv Mater 2016;17:220–228.

9. Min X, Emura S, Nishimura T, Tsuchiya K, Tsuzaki K. Microstructure, tensile deformation mode and crevice corrosion resistance in Ti-10Mo-xFe alloys. Mater Sci Eng A 2010;527:5499–5506.

10. Min X, Tsuzaki K, Emura S, Tsuchiya K. Enhancement of uniform elongation in high strength Ti-Mo based alloys by combination of deformation modes. Mater Sci Eng A 2011;528:4569–4578.

11. Zhou Y, Luo D. Microstructures and mechanical properties of Ti-Mo alloys cold-

rolled and heat treated. Mater Charact 2011;62:931–937.
12. Cai M, Lee C, Lee Y. Effect of grain size on tensile properties of fine-grained metastable β titanium alloys fabricated by stress-induced martensite and its reverse transformations. Scr Mater 2012;66:606–609.
13. Zhang S, Zeng W, Zhou D, Lai Y, Zhao Q. The particle stimulated nucleation in Ti-35V-15Cr-0.3Si-0.1C alloy. Mater Lett 2016;166:317–320.
14. Raabe D. Recovery and Recrystallization: Phenomena, Physics, Models, Simulation. Phys Met 2014; 2291–2397.
15. Chen R, Tan C, Yu X, Hui S, Ye W, Lee Y. Effect of TiB particles on the beta recrystallization behavior of the Ti-2Al-9.2Mo-2Fe-0.1B metastable beta titanium alloy. Mater Charact 2019;153:24–33.
16. Chen R, Hui S, Ye W, Yu Y, Mi X, Lee D, *et al.* High-temperature deformation behaviors of Ti-2Al-9.2Mo-2Fe alloy with boron. Rare Met 2017 https://doi.org/10.1007/s12598-017-0908-7.
17. Gutierrez-urrutia I, Li C, Ji X, Emura S, Tsuchiya K. Quantitative analysis of {332} <113> twinning in a Ti-15Mo alloy by in situ scanning electron microscopy. Sci Technol Adv Mater 2018;19:474–483.
18. Cherukuri B, Srinivasan R, Tamirisakandala S, Miracle D. The influence of trace boron addition on grain growth kinetics of the beta phase in the beta titanium alloy Ti-15Mo-2.6Nb-3Al-0.2Si. Scr Mater 2009;60:496–499.